



Cite this: DOI: 10.1039/d5em01010a

## Toxicity assessment of coal ash after 50 years of weathering: the integration of multielement analysis and biological endpoints

Petrović M.,<sup>a</sup> Vidaković-Cifrek Ž.,<sup>b</sup> Medunić G.<sup>b</sup> and Fiket Ž.<sup>a\*</sup>

Coal ash disposal poses a significant environmental risk due to the potential leaching of toxic elements into surrounding ecosystems. Here, we analysed the phytotoxic effect of two coal ash disposal sites after 50 years of weathering to evaluate whether coal ash remains toxic after long-term disposal and whether vegetated areas are less toxic than bare ones. To analyse that, a combination of multielement analysis of coal ash and eluates and two bioassays—seed germination and *Allium* test—was used. Multielement analysis revealed that some samples exceeded the World Health Organization's drinking water thresholds; however, biological responses did not consistently align with the total element concentrations. Seed germination was inhibited in 7 out of 12 samples, most strongly in soil and bare ash eluates from both sites. The *Allium*-based cytogenetic assay showed high mitotic inhibition and genotoxicity in most eluates. Correlation analyses linked Al, As, and V with increased chromosomal aberrations. However, the potential for synergistic or antagonistic interactions among elements complicates the straightforward predictions of toxicity based on concentration alone. Overall, these results advocate for the integration of biological endpoints with chemical data and highlight the persistent toxicity of coal ash even after 50 years of weathering.

Received 5th December 2025  
Accepted 9th April 2026

DOI: 10.1039/d5em01010a

rsc.li/espi

### Environmental significance

Coal combustion residues (CCR) are one of the world's largest industrial waste streams, yet their long-term environmental risks remain poorly understood. This study provides one of the first systematic evaluations of phytotoxicity and genotoxicity from ~50-year-old weathered coal ash deposits. By combining chemical analysis with bioassays, we show that coal ash remains toxic decades after disposal, despite partial natural attenuation through vegetation and pedogenesis. Correlation analyses, supported by mechanistic evidence from the literature, suggest that aluminum, arsenic, and vanadium are likely contributors to the observed chromosomal damage. Biological responses did not consistently align with measured elemental concentrations, highlighting the limitations of relying solely on concentration-based thresholds and emphasize the need for integrated chemical–biological approaches in the management of legacy CCR disposal sites.

## 1. Introduction

Coal combustion residues (CCRs) refer to four materials (fly ash, bottom ash, slag, and flue gas desulfurization by-products) generated as by-products during coal combustion. Approximately 1.1 billion tons of CCRs are produced annually worldwide, out of which 60% is utilized, and the rest is disposed of in surface impoundments.<sup>1</sup> CCRs, excluding the flue-gas desulfurization by-products, consist of non-combustible inorganic materials with varying percentages of unburned coal particles (organic matter) and are enriched in organic pollutants (PAHs) and trace elements.<sup>2,3</sup>

Among these trace elements are naturally occurring radionuclides (*e.g.*, <sup>238</sup>U, <sup>232</sup>Th, and <sup>226</sup>Ra) and potentially hazardous metal(loid)s (*e.g.*, As, Pb, Cd, Cr, Hg, Se, B, and Mo) that exist at 2–10 times higher concentrations than that in the parent coal.<sup>4</sup> When CCR is disposed of in landfills or impoundments, contaminants may leach into surrounding soils and waters, while fine ash particles can get transported over long distances as they are airborne, creating multiple exposure pathways.<sup>5,6</sup>

The toxic effects of CCR both in the field and laboratory settings are well documented. In aquatic and terrestrial systems, coal ash has reduced the swimming speed of toads, leading to higher predation risk;<sup>7</sup> caused oral and spinal deformities in amphibians and fish;<sup>8,9</sup> and contributed to mercury poisoning in cattle that are grazing near coal power plants.<sup>10</sup> Epidemiological investigations have reported associations between proximity to CCR disposal sites and increased respiratory symptoms, developmental concerns and

<sup>a</sup>Ruder Bošković Institute, Bijenička Cesta 54, 10000 Zagreb, Croatia

<sup>b</sup>Faculty of Science, University of Zagreb, Horvatovac 102a, 10000 Zagreb, Croatia.  
E-mail: zeljka.fiket@irb.hr



neurobehavioral problems in children.<sup>11–13</sup> Laboratory bioassays across a wide range of model systems, including plants, invertebrates, microbes, and human cells, have demonstrated that CCR can impair growth, reproduction, and genetic integrity, with dose-dependent effects.<sup>14–19</sup> Collectively, these findings demonstrate that the impacts of CCR extend from microorganisms to higher organisms. These responses are commonly associated with oxidative stress, inflammation, and DNA damage, resulting from the release and bioavailability of enriched metal(loid)s, such as As, Cd, Cr, Pb, Hg, and Se.<sup>15,20–22</sup> However, trace elements, PAHs, radionuclides, and high salinity may act alone or synergistically, making it difficult to pinpoint the mechanisms of toxicity.<sup>23,24</sup>

Moreover, the magnitude of the toxic effects depends strongly on the ash composition, which can differ significantly even among ashes from the same power plant.<sup>5</sup> Because the ash composition governs toxicity, understanding how it changes under environmental conditions is essential.

Over time, CCR does not remain chemically static. After disposal, decade-long weathering processes alter its physicochemical properties. Reported changes include a decline in pH (from ~12 to <9), secondary mineral precipitation (*e.g.*, calcite), and an increase in organic matter.<sup>25,26</sup> These transformations affect pollutant release<sup>27</sup> and, consequently, toxicity. Yet, most CCR are assessed before disposal, even though landfills worldwide are now several decades old and continue to evolve. Understanding the toxicity of weathered CCR is therefore essential for long-term risk assessment.

To date, few studies have addressed the toxicity of weathered CCR. For example, Bandarra *et al.*<sup>28</sup> tested weathered CCR eluates on five organisms (the plant *Lepidium sativum*, the bacteria *Alivibrio fischeri*, the microalgae *Raphidocelis subcapitata*, the macrophyte *Lemna minor* and the microcrustacean *Daphnia magna*) and found overall low impairment, with *Daphnia magna* being the most sensitive. Toxicity was reduced after pH adjustment, underscoring the influence of weathering. Still, systematic evaluations of weathered CCR remain rare, despite the global prevalence of old CCR disposal sites.<sup>29</sup>

Both landfills investigated in this study are Croatian CCR disposal sites, each comprising a mosaic of bare ash deposits and vegetated areas that have undergone differing degrees of weathering and early pedogenesis.<sup>26</sup> Vegetated zones exhibit lower pH levels, greater secondary mineral formation, and higher organic matter content compared to adjacent bare or cemented deposits, which retain properties resembling fresh ash. In our previous work, we demonstrated that this pronounced spatial heterogeneity results from cementation processes and early soil formation developing over the past ~50 years.<sup>26</sup> These contrasting conditions within each landfill provide a natural framework for comparing the toxicity of differently weathered CCR materials exposed to the same climate and deposition history.

In this study, we investigated two legacy Croatian CCR landfills using two phytotoxicity assays: the seed germination test and the *Allium* test, following established procedures widely used in environmental monitoring.<sup>30–32</sup> The seed germination assay evaluates phytotoxicity by measuring the

inhibition of germination and early root elongation, providing a sensitive indicator of plant-level stress caused by CCR exposure. Because germination and early root growth represent the first stages of plant establishment, this assay is particularly relevant for assessing how vegetated and bare areas differ in their ability to support plant growth. The *Allium* test assesses cytotoxic and genotoxic effects in actively dividing root meristem cells through mitotic index and chromosomal aberration endpoints. This allows the evaluation of whether CCR exposure disrupts normal cell division and induces chromosomal damage.

Therefore, we aim to (1) assess the toxicity of ~50-year-old weathered CCR, (2) test whether vegetated areas are less toxic than bare deposits, and (3) evaluate statistical associations between toxicity endpoints and trace element concentrations using correlation analyses to identify which elements are most likely contributing to toxicity. Because experimental testing of individual chemical species in isolation was beyond the scope of this study, these correlations serve as an informative first step toward identifying potential toxic contributors. By addressing these aims, we provide new insight into the long-term evolution of CCR toxicity and its implications for the management and rehabilitation of legacy disposal sites.

## 2. Materials and methods

### 2.1. Study area

This study focuses on two unlined CCR landfills located in Štrmac and Plaški villages in Croatia (Europe) (Fig. 1).

The first landfill (LŠ) is situated in Štrmac, a village on the Istrian peninsula, western Croatia (Fig. 1b). It covers ~17 000 m<sup>2</sup> and consists of coal bottom ash and slag disposed of by a local foundry in the 1960s. The nearest residents live only ~12 m away. The top of the landfill is planted with conifers, while the slopes remain largely bare, with patches of grass and other pioneer species. The ash was produced by burning local Raša coal, a super-high-organic-sulfur coal enriched in S, Se, Mo, U, V, and Re.<sup>33,34</sup> A detailed description of the geological and geochemical characteristics of Raša coal can be found elsewhere (Medunić *et al.*, 2018; Medunić *et al.*, 2016), as well as environmental pollution caused by its combustion.<sup>22,35,36</sup>

The second landfill (LP) is situated in Plaški, a village in the Lika Region (Fig. 1c). The landfill consists of 70 000 m<sup>3</sup> of fly and bottom ash disposed of by the former sulfate pulp factory operating from 1965 to 1991. The height of the landfill varies from 3.5 to ~13 m.<sup>37</sup> The top of the landfill is covered with naturally growing grass, while the slopes are bare, with patches of pioneer plant species (Fig. 1c). Slopes are cemented, which is often found in such landfills.<sup>38</sup> The type of coal burned in the factory is publicly unknown.

A detailed characterization of the physicochemical and mineralogical properties of the samples from these two landfills, including granulometric characteristics, distribution of mineral phases, cation exchange capacity, and particle surface area, can be found in the study by Petrović *et al.*<sup>26</sup> According to this study, the bare section of the Štrmac landfill is primarily influenced by abiotic processes (the second stage of landfill



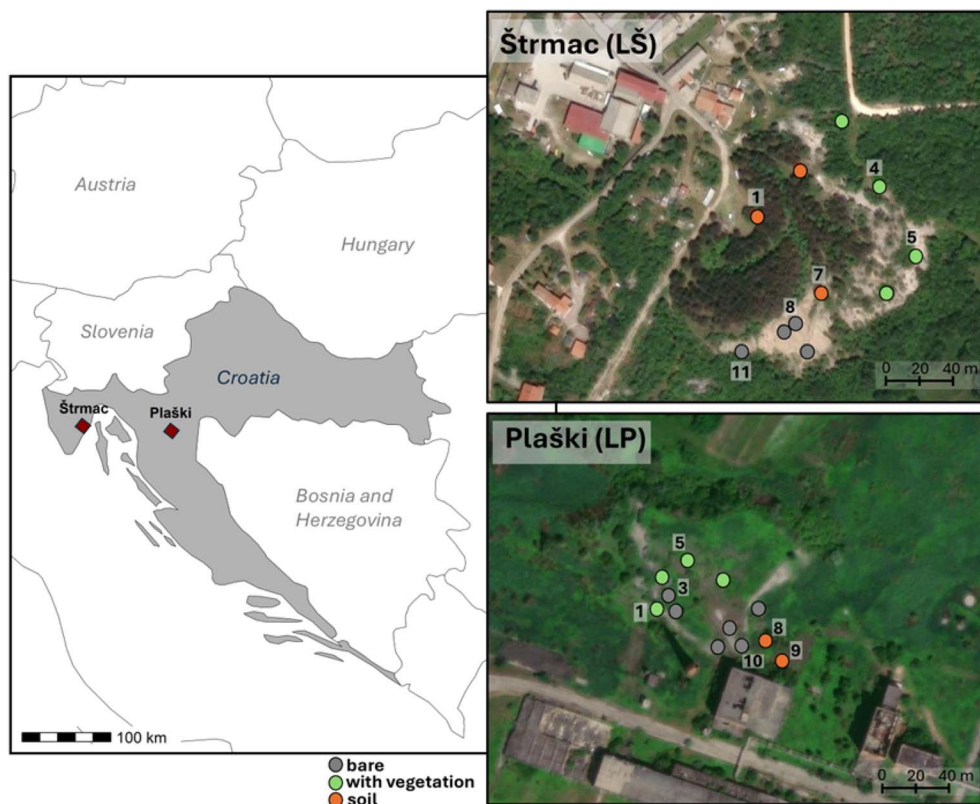


Fig. 1 Study area adapted from Petrović *et al.*<sup>26</sup> showing the locations of the two landfills in Croatia and the sampling sites at Štrmac (LŠ) and Plaški (LP) landfills. At each location, several samples with varying depths were taken, and the ones with visible numbers were used for the phytotoxicity study. The physicochemical and mineralogical characteristics of all collected samples are presented in Petrović *et al.*<sup>26</sup> Note: an LP1 sample is an intermediate sample. Chemically, it resembles a bare sample, and the grass did not fully cover it like it did the rest of the samples 'with vegetation'. However, that area had patches of vegetation growing on it; thus, in this study, it was classified as a sample with vegetation.

evolution), while the vegetated areas exhibit early signs of pedogenesis (the third stage). In contrast, both the bare and vegetated samples of the Plaški landfill show signs of early pedogenesis (3rd stage).

## 2.2. Sampling and sample preparation

The sampling campaign was conducted in July 2020 (LŠ) and May 2021 (LP) with a total of 69 samples collected. The sampling details and sample preparation can be found in Petrović *et al.*<sup>26</sup> For the total element analysis, all samples were analyzed. For phytotoxicity testing, 12 samples were chosen (6 from both landfills), including soil samples (LŠ1, LŠ7, LP8, LP9), naturally vegetated samples (LŠ5, LŠ4, LP5, LP1) and bare samples (LŠ8, LŠ11, LP3, LP10). In addition, an *Allium* test was performed on two "fresh" ash samples (fly ash, FA and bottom ash, BA) generated, collected, and properly stored in the 1970s from the Plomin Thermal Power Plant, which used the same Raša coal as the foundry in Štrmac.

**2.2.1. Sample preparation for the total element analysis.** For the total element analysis, sub-samples (0.05 g), previously homogenized in an agate mill, were subjected to a total digestion in the microwave oven (Multiwave 3000, Anton Paar, Graz, Austria) in a two-step procedure. The latter involved digestion

with a mixture of 4 mL of nitric acid ( $\text{HNO}_3$ , 65%, pro analysi, Kemika, Zagreb, Croatia), 1 mL of hydrochloric acid (HCl), and 1 mL of hydrofluoric acid (HF, 48%, pro analysi, Kemika, Zagreb, Croatia), followed by the addition of 6 mL of boric acid ( $\text{H}_3\text{BO}_3$ , Fluka, Steinheim, Switzerland). Prior to analysis, digests were 10-fold diluted, acidified with 2% (v/v)  $\text{HNO}_3$  (65%, supra pur, Fluka, Steinheim, Switzerland), and In ( $1 \mu\text{g L}^{-1}$ ) was added as the internal standard.

**2.2.2. Eluate preparation.** A standardized European leaching batch test (EN-12457-2) at a liquid to solid ratio of 10 : 1 was used for eluate preparation.<sup>39</sup> The prepared suspensions were shaken for 24 h using the mechanical shaker at 320 rpm, centrifuged, and filtered using a  $0.45 \mu\text{m}$  filter. Since some samples have very high pH (>11), the pH of the eluates was adjusted to 6–7 with 1 M, 0.5 M, and 0.1 M HCl to remove pH as a toxic parameter and focus on ash constituents (Table S1).

## 2.3. Multielement analysis

Elemental concentrations were determined by inductively coupled plasma triple quadrupole mass spectrometry (ICP-QQQ, 8900 Agilent, USA). A total of 30 elements were analysed: Al, As, Ba, Be, Bi, Ca, Cd, Co, Cr, Cs, Cu, Fe, K, Li, Mg, Mn, Mo, Na, Ni, Pb, Rb, Sb, Se, Sn, Sr, Ti, Tl, U, V, and Zn.



Analytical quality control included procedural blanks, instrument blanks, and repeated analysis ( $n = 6$ ) of certified reference materials (CRMs). Three CRMs were used to verify the analytical performance across different matrices: NCS DC 77302 (China National Analysis Centre for Iron and Steel, Beijing, China) for soil samples, NCS FC 28145 (China National Analysis Centre for Iron and Steel, Beijing, China) as a certified coal ash reference material, and SLRS-4 (National Research Council Canada) for aqueous eluate analyses.

Recoveries for all elements ranged between 90% and 110% of certified values. The relative standard deviations (RSD) for the CRM replicate analyses were generally below 5%. Instrument blanks were consistently below the detection limits for all measured elements. The limits of detection (LOD) were calculated as three times the standard deviation of repeated procedural blank measurements and are reported in the Tables S4 and S6.

The results of total analysis for As, Cr, Mo, Se, U, and V were reported previously for the interpretation of leaching tests.<sup>27</sup> The total concentration for the rest of the elements and the eluate concentrations have not been previously published. The results of the eluates were compared to the EU non-hazardous landfill leachate limits<sup>40</sup> and the more rigid WHO/EU drinking water thresholds.<sup>41</sup>

## 2.4. Ecotoxicity testing

**2.4.1. Seed germination test.** The germination test was performed according to the procedures described in Fritz *et al.*<sup>42</sup> (2007) and Luo *et al.*<sup>32</sup> (2018) with certain modifications. Two layers of sterile filter paper and 5 mL of the sample or 5 mL of pure water (Milli-Q), which we used as a negative control, were added to sterile plastic Petri dishes with a diameter of 9 cm. 20 lettuce seeds (*Lactuca sativa* L., a variety of Dalmatian ice lettuce) were placed in each bowl. Four replicates for each sample investigated were left in the dark at a temperature of  $22 \pm 1$  °C. For four days (96 h), we recorded the number of germinated seeds. To maintain humidity, on the third day of the experiment (after 72 h), we added another 2.5 mL of the sample, or Milli-Q water (control), to the Petri dishes. At the end of the fourth day of the experiment (96 h), we measured two toxicity endpoints: seed germination and radicle length.<sup>42</sup>

We expressed the results as follows:

(a) Seed germination (SG): the percentage of germinated seeds in a certain period of time:

$$SG(\%) = \frac{\text{no. of germinated seeds}}{\text{no. of total seeds}} \times 100$$

(b) Relative seed germination (RSG): the percentage of germinated seeds in the treatment compared to the control (used only to calculate the Germination index):

$$RSG(\%) = \frac{\text{no. of germinated seeds}(\text{sample})}{\text{no. of total seeds}(\text{control})} \times 100$$

(c) Relative radicle growth (RRG): the length of the radicle after the treatment compared to the length in the control:

$$RRG(\%) = \frac{\text{radicle length in treatment}}{\text{radicle length in control}} \times 100$$

(d) Germination index (GI):

$$GI = \frac{RSG \times RRG}{100}$$

**2.4.2. Allium test.** Onion bulbs (*Allium ascalonicum* L.), with ~2 cm diameter, were prepared by removing the dry outer scales and gently cleaning the base of each bulb without damaging the root primordia. The bulbs were placed on the top of glass flasks filled with reverse osmosis-purified tap water (pH 6.5), and roots were allowed to grow for 48 hours, with daily water changes. Once the roots reached ~1.5 cm, the bulbs were exposed for 24 hours to sample eluates, with five biological replicates per treatment. Tap water was used as the negative control, and a  $5 \mu\text{mol L}^{-1}$  copper sulfate solution ( $\text{CuSO}_4 \times 5 \text{H}_2\text{O}$ ) was used as the positive control.

After treatment, some roots were fixed immediately in ethanol-acetic acid (3 : 1), while others were placed in fresh tap water for a 24-hour recovery before fixation. All procedures were carried out at  $22 \pm 1$  °C and shielded from light. It should also be noted that the tap water used during root growth, the recovery period, and as a negative control was left at room temperature for 24 hours and aerated for at least 5 minutes before use in the experiment. During the experiment, the water was changed every 24 hours.

Fixed roots were hydrolyzed in 1 M HCl (Lach-Ner s.r.o.) at 60 °C for 10 minutes and stained with Schiff's reagent<sup>43</sup> for 1.5 hours. The roots were then prepared for microscopy by immersing the meristem region in a drop of 45% (v/v) glacial acetic acid. The meristem region was then cut off, and the tissue of the root tip was crushed with a glass rod, covered with a coverslip and pressed with the thumb ("squash" technique). At least five microscope slides were prepared per treatment, and a minimum of 4000 cells were analyzed per condition using a Primo Star Zeiss light microscope under 40× or 100× magnification. The following parameters were determined:

(a) Mitotic index (MI): the percentage of dividing cells in the total number of observed cells:

$$MI(\%) = \frac{\text{no. of dividing cells}}{\text{no. of total cells}} \times 100$$

(b) Chromosomal aberrations (CA): the percentage of cells with chromosomal or mitotic aberrations in the total number of cells in division:

$$CA(\%) = \frac{\text{no. of cells with aberrations}}{\text{no. of cells in division}} \times 100$$

In addition, the types of chromosomal aberrations were recorded.



## 2.5. Statistical analyses

All values are obtained from four replicates. Unless otherwise stated, descriptive values in the text refer to sample means. Boxplots in all figures display medians and interquartile ranges. Statistical analyses were performed in MATLAB R2023b.

Differences among treatments were evaluated separately for each landfill (Štrmac and Plaški). For the seed germination test, one-way ANOVA, followed by Tukey's *post hoc* test, was performed, including all eluate treatments and the corresponding negative control within each site. For the Allium test, separate one-way ANOVAs were conducted for the mitotic index (MI) and chromosomal aberrations (CA), including all exposure treatments and controls within each site. Recovery-phase data were analyzed independently using the same approach. The significance level was set at  $p < 0.05$ .

Spearman correlation coefficients were calculated for biological endpoints and eluate concentrations, and the results were visualized as heatmaps.

## 3. Results and discussion

### 3.1. Geochemical characterization of weathered coal ash samples

The geochemical composition of major oxides in CCR samples was assessed using concentration coefficients (CC), defined as the ratio between measured oxide concentrations and the average composition of European coal ash. This approach highlights the relative enrichment (CC > 1) or depletion (CC < 1) of elements compared to the typical European CCR.<sup>44</sup>

The results revealed the high enrichment of sulfur and calcium and the depletion of other oxides ( $\text{Al}_2\text{O}_3$ ,  $\text{Fe}_2\text{O}_3$ ,  $\text{K}_2\text{O}$ ,  $\text{MgO}$ ,  $\text{MnO}$ ,  $\text{Na}_2\text{O}$ ,  $\text{P}_2\text{O}_5$ , and  $\text{TiO}_2$ ) (Fig. 2). A high sulfur enrichment in Štrmac CCR reflects their origin from Raša coal, a unique coal type with exceptionally high organic sulfur content.<sup>33,45,46</sup> Similarly, CaO enrichment and the depletion of  $\text{Al}_2\text{O}_3$  and  $\text{Fe}_2\text{O}_3$  were expected, given the abundance of Ca-bearing minerals, such as calcite ( $\text{CaCO}_3$ ), gypsum ( $\text{CaSO}_4 \cdot 2\text{H}_2\text{O}$ ), portlandite ( $\text{Ca(OH)}_2$ ), and ettringite ( $\text{Ca}_6\text{Al}_2(\text{SO}_4)_3(\text{OH})_{12} \cdot 26\text{H}_2\text{O}$ ) in these ashes.<sup>26,46</sup>

These oxide patterns have important implications for ash reactivity, as they classify both ashes as Ca-rich ash (class C).<sup>47</sup> Ca-rich ashes typically have high buffering capacity, alkaline pH, and a tendency to leach oxyanion-forming elements, such as As, Cr, Mo, P, S, Se, Sb, U, and V.<sup>46</sup>

The CC of the trace elements in the coal ash samples, normalized to world coal ash averages,<sup>48</sup> revealed clear patterns of enrichment and depletion across the two landfill sites and material types (Fig. 3). At Plaški, high enrichment was observed for Ni, Cr, and U, with moderate enrichment of V, Mo, and Cs. At Štrmac, similarly high values were recorded for Mo and U, along with relatively greater enrichment of Se compared to the case at Plaški. In contrast, unweathered ash samples (FA and BA) showed enrichment in Rb (6.4) and Mo (3.1), together with consistently higher CCs for several alkali metals compared to weathered landfill materials (Table S5).

When comparing different sample types (bare and with vegetation), the Plaški samples displayed a more uniform distribution, with bare ash consistently enriched in most trace elements. At

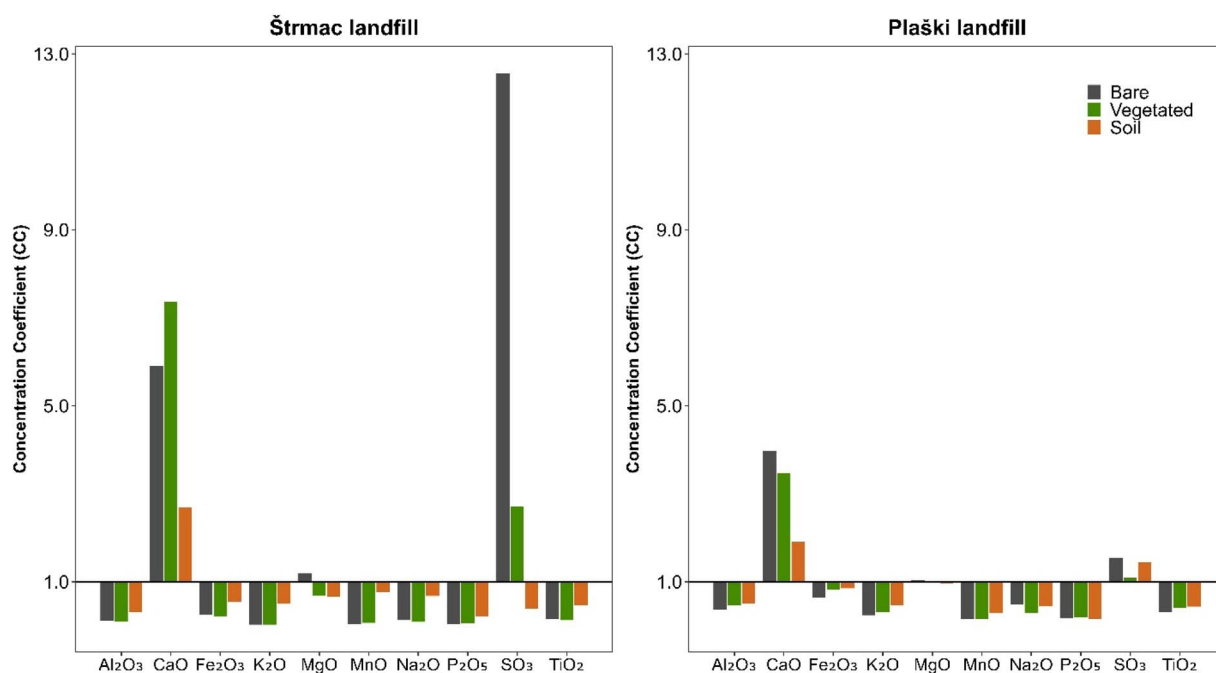


Fig. 2 Median concentration coefficients (CC) of major oxides in the samples from the Štrmac and Plaški coal combustion residue (CCR) landfills. CC was calculated as the ratio of the oxide concentration in each sample type to the average oxide concentration in European coal ash.<sup>44</sup> Values above 1 indicate enrichment, while values below 1 indicate depletion. Total oxide concentrations for each sample are reported in the SI (Tables S2 and S3).



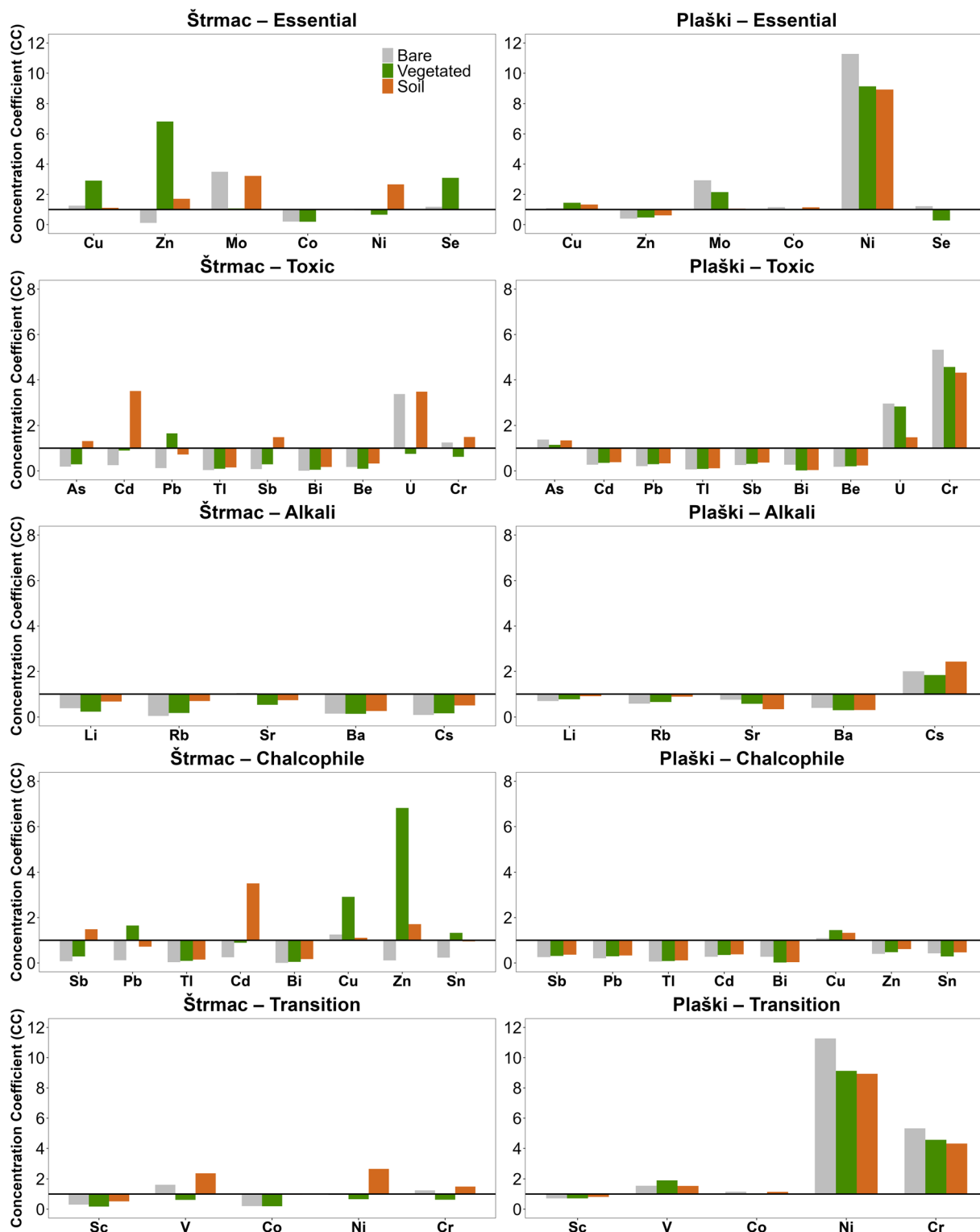


Fig. 3 Average concentration coefficients (CC) of trace elements in the Štrmac and Plaški samples. CC was calculated as the ratio of the sample element concentration to the global coal ash average.<sup>48</sup> Elements were grouped by plant relevance (essential vs. toxic) and geochemical behaviour (alkali, transition and chalcophile) to highlight mobility and uptake pathways.<sup>49,50</sup> Categories are not mutually exclusive; hence, some elements appear in more than one group. Full concentrations are in the SI (Tables S4 and S5).

Štrmac, the distribution was less uniform, where ash with vegetation showed higher enrichment in Cu, Zn, and Se, and soil materials in Ni and Cd, compared to the bare ash samples.

### 3.2. Geochemical characterization of ash leachates

Although the analyzed samples were enriched in several major and trace elements compared to the European and global



averages, the total concentration alone does not reflect the toxic capacity of coal ashes. To better assess the environmental risk, the relative mass leached (RML, %) and water-soluble concentrations were determined.

Most major and trace elements showed low mobility (RML < 1%), indicating strong retention in the solid phase. However, several elements exhibited much higher release, depending on the sample type and site conditions. Among major elements, Na, K, and Ca were the most mobile. Na reached 22.6% in LP3 and 16.1% in BA, with elevated values also in FA (7.9%), LŠ1 (5.5%), and LŠ11 (6.4%). K peaked in LŠ4 (27.4%) and LŠ8 (13.5%), while Ca was highly soluble in BA (24.0%). Mg was generally stable, except in LP3 (5.6%) (Table S7). These values are consistent with the dissolution of soluble salts and Ca-bearing phases, such as gypsum ( $\text{CaSO}_4 \cdot 2\text{H}_2\text{O}$ ), portlandite ( $\text{Ca}(\text{OH})_2$ ), and ettringite ( $\text{Ca}_6\text{Al}_2(\text{SO}_4)_3(\text{OH})_{12} \cdot 26\text{H}_2\text{O}$ ), which are typical of high-Ca ashes.<sup>26,46,51,52</sup>

Among trace elements, the highest mobilities were observed for Cd, Mo, Pb, Zn, Sr, and Se (Fig. 4 and Table S7). Cd was highly mobile in LP3 (21.6%) and BA (24.0%). Mo reached 22.6% in LP3 and was also elevated in LŠ1 (5.5%) and LŠ11 (6.4%). Pb showed moderate release in LP3 (5.1%). Zn reached 11.5% in LŠ11 and 8.9% in BA. Sr was especially mobile in FA (9.5%), while Se was enriched in BA (15.2%) and FA (6.4%). In contrast, Ni remained consistently low (<0.5%) in all samples, despite its enrichment in Plaški ashes.

Clear differences were observed between sample types. Bare ashes (LP3, LŠ11) and unweathered ashes (FA, BA) consistently showed the highest leaching fractions, reflecting the dominance of soluble phases, typical of the early abiotic stage of landfill evolution.<sup>26</sup> Within this group, individual samples, such as LP3 and LŠ11, showed especially high leaching fractions. This variability between the same sample type may be linked to localized cementation, which could have reduced infiltration and promoted the accumulation of soluble salts in parts of the landfill, similar to cementation zones described in mine tailings.<sup>53</sup>

In contrast, vegetated or soil samples (LP1, LP5, LŠ7, LŠ5) generally showed lower RML values than bare samples. Lower RML values in vegetated samples are likely a result of more advanced pedogenesis in those samples.<sup>26</sup> A decrease in pH to a more neutral value, a higher organic matter content, and the precipitation of more stable secondary minerals (calcite, clays) may all have caused the reduction in element release.<sup>54</sup> However, some unexpected results were observed, including more mobile As in the vegetated Plaški sample (LP5) and U, As, and V in the vegetated Štrmac samples. Unlike cationic elements (*e.g.*, Pb, Zn, and Ni), which are strongly retained by clays, oxides, and organic matter, these elements occur mainly as oxyanions (arsenate, uranyl-carbonate, vanadate). The shift from hyper-alkaline conditions in bare ash to neutral-alkaline conditions in vegetated samples<sup>26</sup> may have promoted higher release of the mentioned oxyanion species. This has been observed in modelling studies of the leaching of oxyanion species from coal ash<sup>55</sup> and our previous leaching study, which showed that pedogenesis changes how As and V are released.<sup>27</sup> Thus, while vegetation and soil development generally reduce trace element

release, they may simultaneously promote the mobility of certain oxyanion-forming elements.

Site-specific differences were also evident. Plaški samples were more prone to releasing oxyanion-forming elements (As, V) and alkali metals (Li, Rb). In contrast, Štrmac samples released more Ba, Ca, Sr, Cr, and Cu, likely reflecting the Raša coal origin and the abundance of soluble Ca-S phases that favor co-leaching of alkaline earths and redox-sensitive trace metals under strongly alkaline conditions.<sup>36,45</sup>

Overall, element mobility appears to be governed by both the stage of pedogenesis and site-specific mineralogy, with cementation and salt accumulation offering explanations for localized hotspots, such as LP3. Bare and unweathered ashes (LP3, LŠ11, FA, BA) exhibited the highest leaching, while soil and vegetated samples were more stable, with exceptions in certain oxyanion-forming species. These findings highlight the role of landfill evolution, cementation, and coal origin in determining which elements remain environmentally relevant during long-term weathering of CCR.

**3.2.1. Comparison with environmental standards.** To further assess the risk and describe the samples' composition, elemental concentrations were compared to two regulatory thresholds commonly used for comparison in leaching studies.

When compared to the EU non-hazardous landfill leachate limits,<sup>40</sup> most eluate concentrations were below regulatory thresholds. Only Mo in one sample (LP3, bare) exceeded the EU limits for non-hazardous waste leachate. No other sample exceeded these limits; therefore, from a waste classification perspective, almost all samples would be considered acceptable for disposal at non-hazardous waste facilities.

When applying the more stringent drinking water standards,<sup>41</sup> multiple exceedances were observed (Table 1). The As concentrations exceeded the  $10 \mu\text{g L}^{-1}$  threshold in four Plaški samples (LP1, LP3, LP5, LP8), while Cd was above the  $3 \mu\text{g L}^{-1}$  guideline in LP3. The Cr and Pb levels surpassed their respective drinking water limits ( $50 \mu\text{g L}^{-1}$  and  $10 \mu\text{g L}^{-1}$ ) in LP3 and LP5, and Pb also exceeded the limit in Štrmac samples LŠ4 and LŠ11. Mo exceeded the  $70 \mu\text{g L}^{-1}$  limit only in LP3, which also had the highest concentrations of multiple other metals, including U, Sb, and Ba. The U concentrations were also above the drinking water limit ( $30 \mu\text{g L}^{-1}$ ) in LŠ7, and the barium levels exceeded the  $700 \mu\text{g L}^{-1}$  limit in LŠ11.

Despite the relatively low total concentrations for many metals, these findings highlight that several eluates (LP3, LP5, LŠ7, LŠ11, LŠ4) contain trace elements at levels that exceed safe drinking water standards. This suggests potential environmental risks if such eluates were to enter groundwater systems or surface water bodies, especially in scenarios of long-term leaching. This is particularly important because both landfills are unlined.

### 3.3. Phytotoxicity of weathered coal ash

**3.3.1. Influence of weathered coal ash on seed germination and radicle growth.** The potential toxic effects of weathered coal ash eluates and associated soils were evaluated based on three



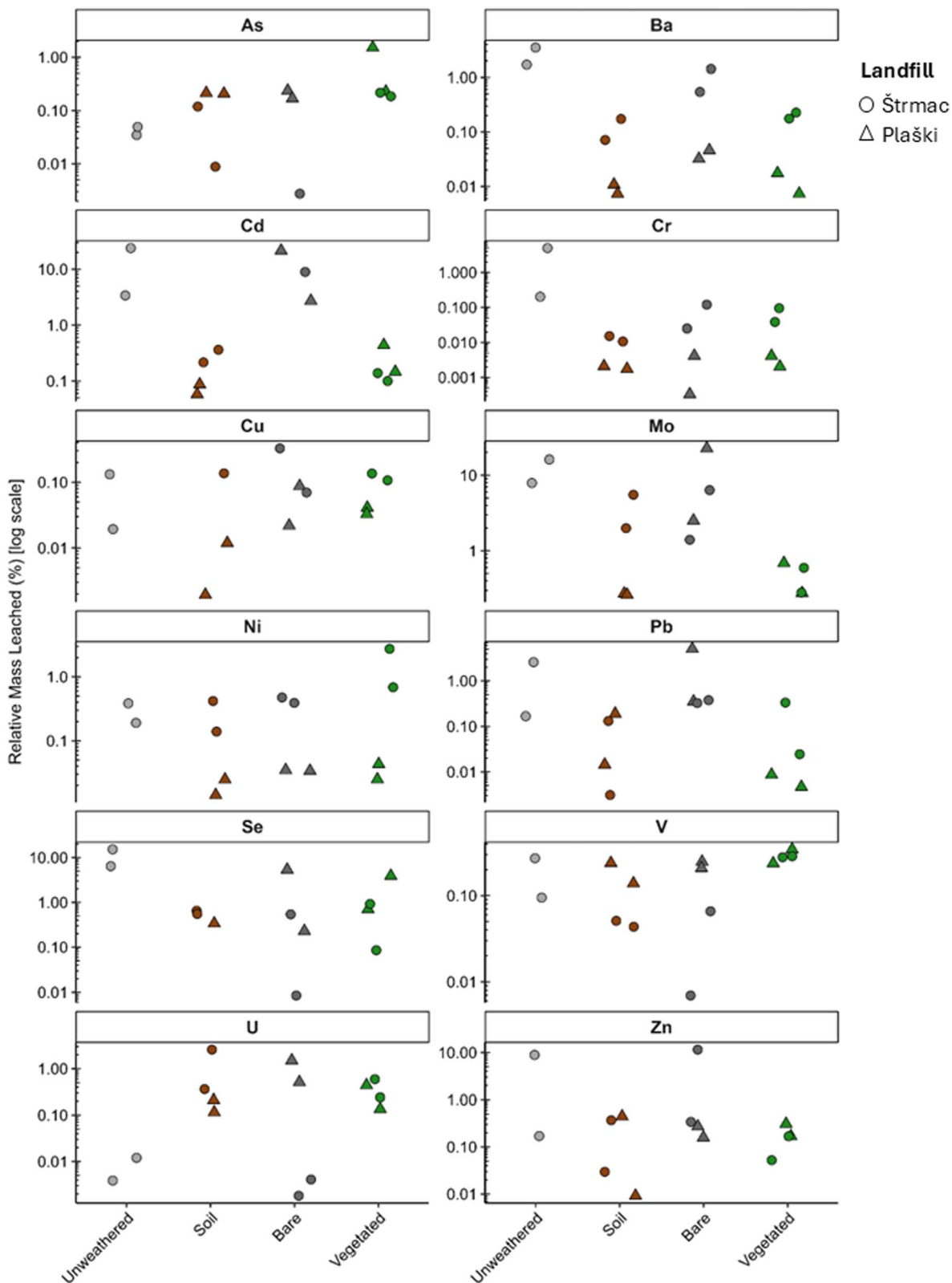


Fig. 4 Relative mass leached (%) of selected trace elements (As, Ba, Cd, Cr, Cu, Mo, Ni, Pb, Se, V, U, and Zn) from coal ash samples in different sample types (unweathered, soil, bare, and vegetated). Values are shown on a logarithmic scale to account for the variation across orders of magnitude. Symbols: Plaški landfill, triangles; Štrmac landfill, circles. Measured concentrations and calculated relative mass leached (RML) values for every element and sample are in the SI (Tables S6 and S7).



**Table 1** Comparison of the measured element concentrations in eluates to two different regulatory thresholds: the EU non-hazardous landfill leachate limits at a liquid-to-solid ratio (L/S) of 10 L kg<sup>-1</sup> (ref. 40) and more rigid WHO drinking water thresholds.<sup>41</sup>

	EU non-hazardous waste leachate limit ( $\mu\text{g L}^{-1}$ )	WHO drinking water limit ( $\mu\text{g L}^{-1}$ )	Minimum ( $\mu\text{g L}^{-1}$ )	Maximum ( $\mu\text{g L}^{-1}$ )	Above limit?	Samples exceeding the limit
As	200	10	0.13	62.5	Yes (4)	LP1, LP3, LP5, LP8
Ba	10 000	1300	5.37	8260	Yes (1)	LŠ11
Cd	100	3	0.01	9.83	Yes (1)	LP3
Cr	1000	50	1.5	98.0	Yes (2)	LP5, LP3
Cu	5000	2000	0.58	132	No	—
Mo	1000	70	0.24	1235	Yes (1)	LP3
Ni	1000	70	11.4	133	Yes (1)	LŠ4
Pb	1000	10	0.06	73.8	Yes (3)	LP3, LŠ4, LŠ11
Sb	70	5	0.03	0.99	No	—
Se	50	40	0.03	6.28	No	—
U	—	30	0.13	276	Yes (2)	LP3, LŠ7
Zn	5000	—	0.25	54.9	No	—

indicators: seed germination, relative radicle growth, and germination index.

Seed germination (SG) of seeds treated with eluates from the Štrmac locality (LŠ1, LŠ4, LŠ5, LŠ7, LŠ8, LŠ11) ranged from 35% to 91%, while for the Plaški samples (LP1, LP3, LP5, LP8, LP9, LP10), it ranged from 20% to 90% (Fig. 5). In comparison, the control seeds germinated at 95%.

Based on ANOVA followed by Tukey's *post hoc* test (Table S8 and Fig. 5), seven of the tested samples showed significant inhibition of germination compared to the control. Among the

Štrmac coal ash samples, inhibition was observed for two bare ash eluates (LŠ8, LŠ11) and one vegetated ash eluate (LŠ5). Among the Plaški coal ash samples, inhibition was observed for two bare ash eluates (LP3, LP10). No significant differences were found between the vegetated and bare ash samples within the Štrmac locality. In Plaški, however, the vegetated ash samples (LP1, LP5) exhibited significantly higher SG than the bare ash samples (LP3, LP10), suggesting early pedogenic effects that mitigate toxicity.

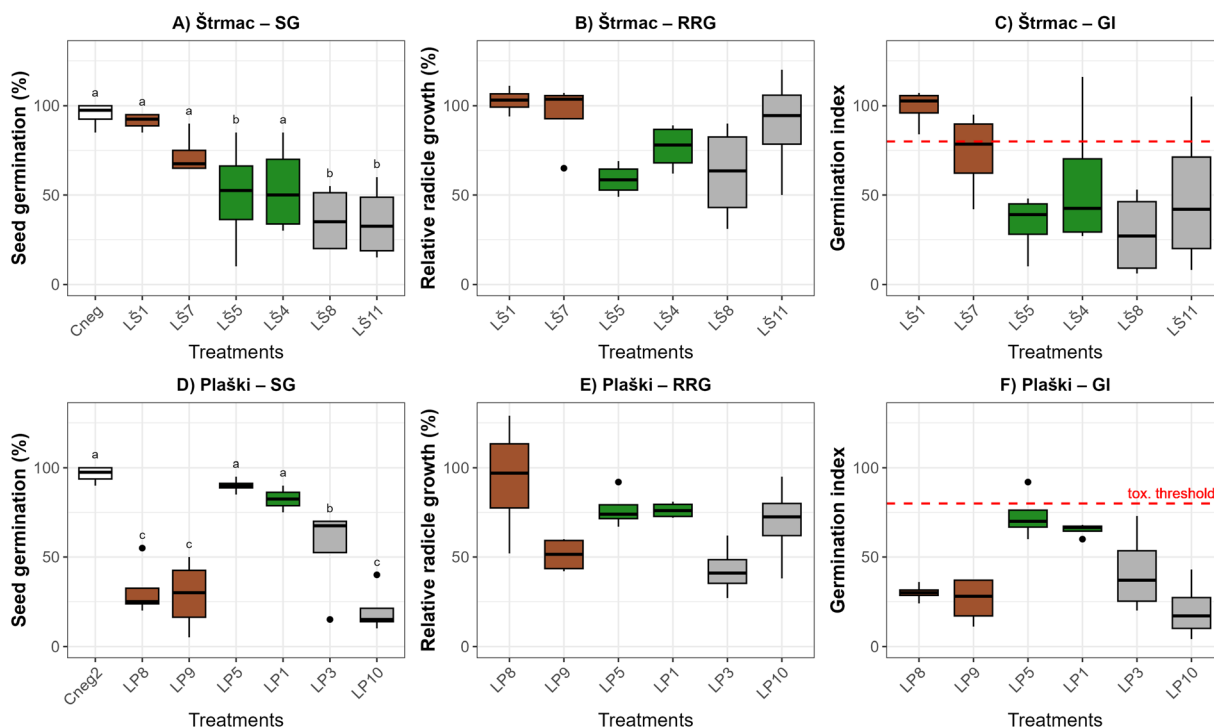


**Fig. 5** Seed germination (%; (A) and (D)), relative radicle growth (%; (B) and (E)), and germination index (C and F) of seeds treated with eluates from the Štrmac (A–C) and Plaški (D–F) localities. Colors denote sample types: negative control (white), soil samples around the landfill (brown), samples with vegetation (green), and bare ash samples (grey). Different lowercase letters above boxplots indicate statistically significant differences between treatments based on one-way ANOVA, followed by Tukey's *post hoc* test ( $p < 0.05$ ). Black dots represent outliers. Based on the literature, a value of 80 was taken as the toxicity threshold (red dashed line) for the germination index.<sup>32</sup>



For soil eluates, significant inhibition was observed in both Plaški soil samples (LP8, LP9), whereas none of the Štrmac soil samples (LŠ1, LŠ7) showed inhibition. The contrasting toxicity patterns most likely stem from differences in sampling locations. Štrmac soils were collected on top of the landfill, whereas Plaški soils were collected downslope beneath the ash body, where leachate accumulation is expected to be greater.

Because radicle growth is a more sensitive indicator of stress,<sup>56,57</sup> it is commonly evaluated for samples that do not significantly inhibit seed germination. The relative radicle growth (RRG) incorporates negative control into its calculation; therefore, values below 100% reflect reduced radicle growth.

Among the Štrmac samples without significant effects on SG (LŠ1, LŠ7, LŠ4), the RRG values varied considerably. Soil samples LŠ1 and LŠ7 showed radicle growth close to the reference level (100%), whereas the vegetated LŠ4 sample exhibited a noticeable reduction. A similar pattern was observed for Plaški. Although vegetated samples LP5 and LP1 did not significantly inhibit SG, both displayed reduced RRG.

These findings demonstrate that germination alone may underestimate toxicity, as radicle growth can be impaired even when seeds germinate successfully. This highlights radicle growth as an important complementary indicator for identifying sublethal effects that may disturb seedling growth and development.

It is worth noting that the samples that inhibited seed germination had a relative radicle growth similar to or even higher than the samples that did not inhibit seed germination, which seems contradictory. For example, two bare samples from both localities, LŠ11 and LP10, had the lowest seed germination of all samples at their respective location, but their radicles were among the longest. Although it could be that some ash constituents only affect seed germination and not radicle growth, it is more likely that the cause is stress-induced growth,<sup>58</sup> particularly because the radicles were visually more twisted and thinner than radicles from the control group. This may be an adaptive mechanism of the plant to explore a larger soil volume to find less toxic zones or more nutrients, or it may be caused by some other effect (e.g., alteration of hormonal balance in the radicles),<sup>59</sup> which future studies should address.

To integrate both germination and radicle growth effects, the germination index (GI) was calculated as it comprehensively reflects the toxicity of the sample.<sup>32,60</sup> For seeds treated with the Štrmac samples, the germination index ranged from 28 to 99, and for the seeds treated with the Plaški samples, the values ranged from 20 to 73 (Fig. 5). Seeds treated with LP10 (20), LŠ8 (28) and LP8 (30) had the lowest indices, and those treated with samples LŠ1 (99), LŠ7 (73), and LP5 (73) had the highest germination indices, showing that toxicity varied among samples.

A GI value of 80 is commonly used as a toxicity threshold; therefore, values above 80 indicate non-toxic conditions, and lower values reflect phytotoxicity.<sup>32,56</sup> Thus, based on this criterion, nine out of twelve samples were classified as toxic. In the Štrmac locality, two bare samples (LŠ8 and LŠ11) and two vegetated (LŠ4 and LŠ5) were classified as toxic, while the soil samples were the least affected. All Plaški samples exhibited GI

< 80, with vegetated samples LP5 (73) and LP1 (65) showing milder toxicity than bare ash eluates LP3 (42) and LP10 (20).

Although most samples showed phytotoxic effects, the severity of toxicity varied between sample types and localities. At Štrmac, the vegetated and bare ash eluates exhibited similar toxicity levels, while at Plaški, the vegetated samples displayed substantially higher GI values, indicating that early pedogenesis has already moderated toxicity in certain parts of the landfill.

Taken together, these results show that early pedogenesis can measurably reduce phytotoxicity, not only through geochemical changes, such as pH buffering, reduced salinity, and secondary mineral formation (see Section 3.2), but also by lessening biological impacts on germination and early root growth (higher GI, higher RRG where SG is unaffected). In other words, pedogenesis at Plaški is already translating into reduced biological stress, even though exceptions remain (e.g., oxyanion-forming elements discussed above). This highlights that landfill evolution influences both geochemical properties and ecological outcomes for the resident biota.

### 3.4. Influence of weathered coal ash on the cell division and chromosomes of *Allium ascalonicum* root tips

The *Allium ascalonicum* root-tip assay revealed that exposure to weathered coal ash caused notable suppression of cell division and induced a spectrum of chromosomal abnormalities in the root meristems. These effects varied by sample type and site of origin, and clear differences were observed before vs. after a recovery period in clean water. The results are detailed below, along with a discussion of their implications and mechanisms.

**3.4.1. Cytotoxicity of weathered coal ash.** Microscopic observations of the *A. ascalonicum* meristematic root tip cells revealed differences in cell division between the negative control and roots treated with the ash (Fig. 6 and Table S8). 11 out of 14 samples significantly lowered cell division compared to the negative control, with the average mitotic index ranging from 1.94% to 4.53%. The highest inhibition of cell division was caused by the vegetated LP1 sample (MI = 1.94%), followed by two unweathered fly (FA) and bottom (BA) ash samples (2.36 and 2.56%, respectively). Soil LŠ1, vegetated LŠ4, and bare LP10 samples did not cause a significant difference in cell division compared to the negative control. For comparison, the mitotic indices of the bulbs treated with the negative and positive controls were 6.03% and 0.35%, respectively (Fig. 6).

A decrease in MI is a well-established indicator of cytotoxicity, reflecting cell-cycle arrest or prolongation of specific phases due to toxic stress. Reduced MI indicates that fewer cells are able to progress into mitosis under chemical exposure.<sup>61</sup> Comparable responses have been reported for fresh coal fly ash. Jana *et al.*<sup>15</sup> documented a >50% reduction in MI in onion roots exposed to concentrated ash leachates, while Chakraborty *et al.*<sup>14</sup> observed complete growth arrest and severe inhibition of mitotic activity at high ash concentrations. These findings support the interpretation that the reduced MI in our samples reflects inhibition of normal cell-cycle progression. Mechanistically, toxicants commonly present in ash, such as certain metals and metalloids, can delay the G<sub>2</sub>/M transition, disrupt



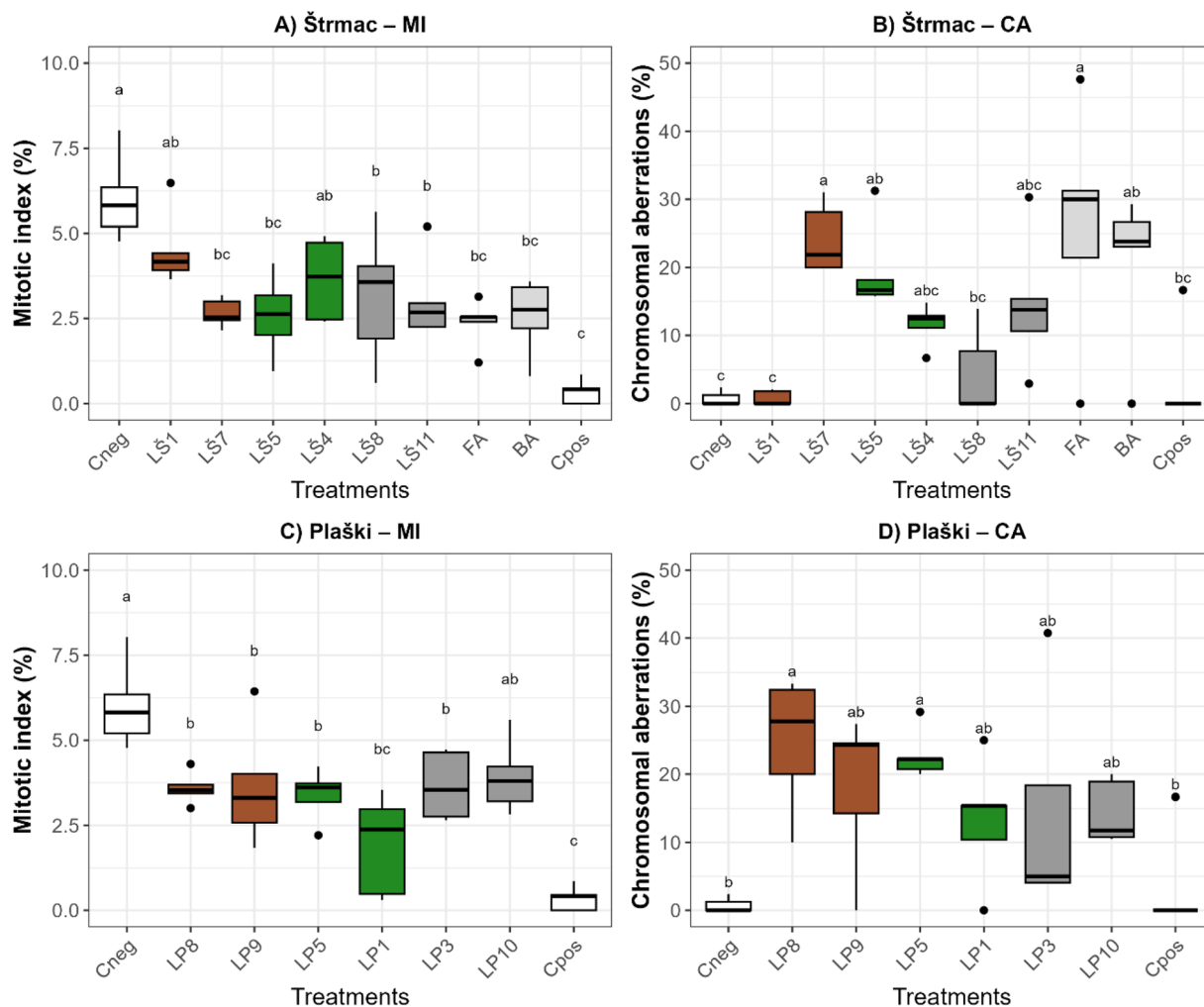


**Fig. 6** Mitotic index (%) and chromosomal aberrations (%) in *Allium ascalonicum* root tips exposed to eluates from Štrmac (A and B) and Plaški (C and D). Panels A and C show mitotic index, and B and D chromosomal aberrations. Colors denote different samples: control (no color), soil samples around the landfill (brown), samples with vegetation (green), and bare samples (grey). Different lowercase letters above boxplots indicate statistically significant differences between treatments based on one-way ANOVA, followed by Tukey's *post hoc* test ( $p < 0.05$ ). Black dots represent outliers.

spindle formation, or activate DNA-damage checkpoints, resulting in fewer cells entering mitosis at any given time.<sup>15,62</sup>

In our study, unweathered FA and BA induced the strongest mitotic suppression, consistent with the higher availability of contaminants in unweathered ash. Weathered samples exhibited a broader range of MI responses, which likely reflects differences in their eluate composition. These relationships are examined in more detail in Section 3.3.

After 24 hours of recovery, which included placing roots in control water and allowing cells to divide under no influence of the leachate sample, cell division increased in all analyzed root tips, with the mitotic index ranging from 2.46% to 5.44%. In comparison, the mitotic indices of the negative and positive controls were 5.36 and 2.97% after recovery, respectively (Fig. 7). All samples, except LP1, LP5, and the positive control, showed an increased MI after recovery compared to their exposure values, indicating that the mitotic inhibition caused by many treatments was at least partially reversible. The reversibility of

MI suppression is commonly interpreted as evidence of acute, non-permanent cell-cycle inhibition rather than irreversible cytotoxic damage, as plants can repair sublethal injuries once the toxicant is removed.<sup>63</sup>

However, not all treatments achieved full recovery. FA remained below the MI of the negative control even after recovery, and LP8 showed a decrease in MI following recovery, suggesting persistent or delayed toxicity. Such patterns may arise when contaminants remain bound within root tissues and continue to affect cell physiology through mechanisms such as oxidative stress or enzyme inhibition, even after external exposure ends.<sup>15</sup>

Overall, the evaluated MI revealed that both unweathered and weathered coal ash eluates can suppress mitotic activity, with varying degrees of reversibility. These data distinguish samples that exert predominantly acute effects from those with more lasting cytotoxic influence.



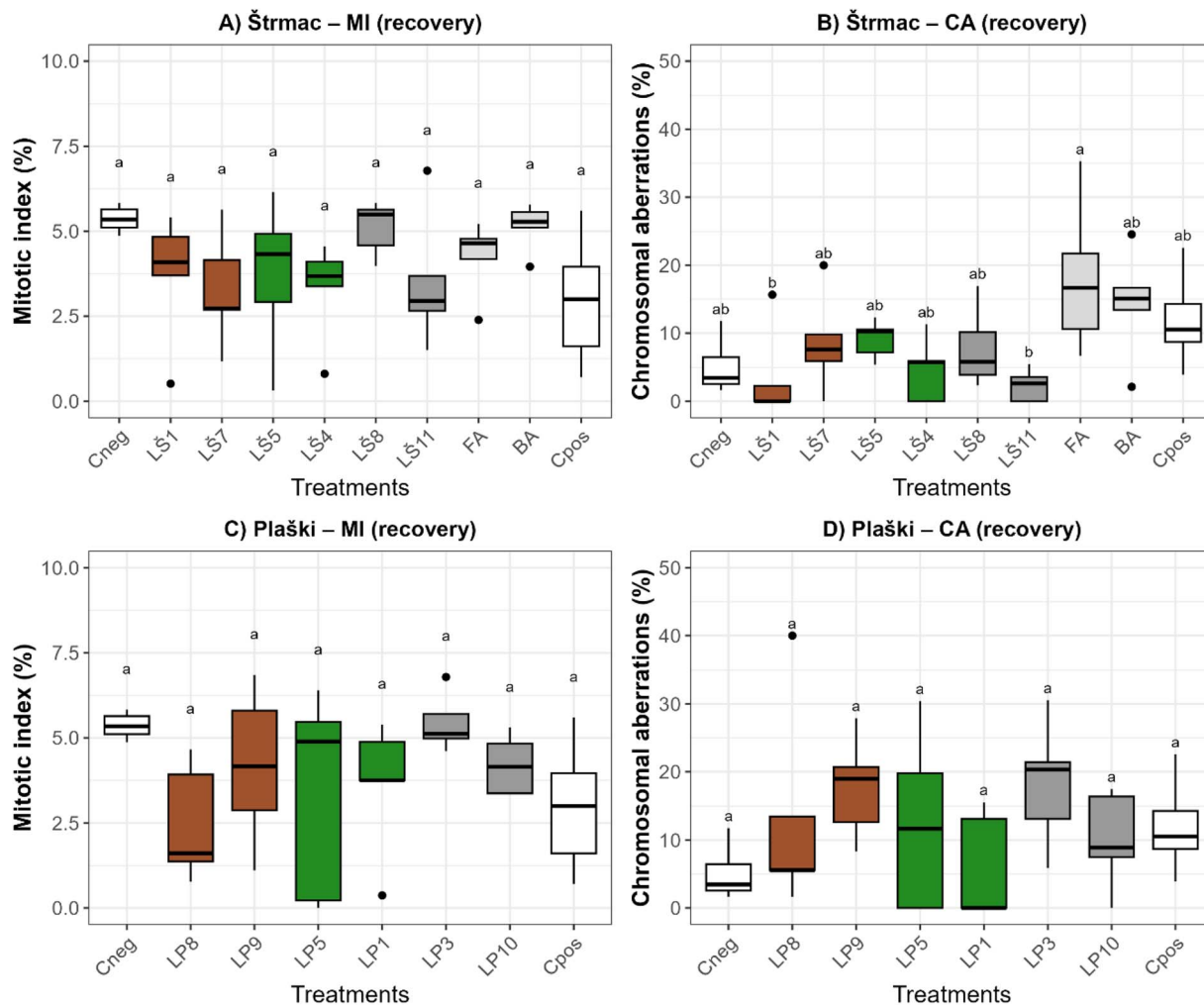


Fig. 7 Mitotic index (%) (A and C) and chromosomal aberrations (%) (B and D) in *Allium ascalonicum* root tips after the 24-h recovery period in water for Štrmac samples (A and B) and Plaški samples (C and D). Boxplots show medians and interquartile ranges; black dots represent outliers. Different lowercase letters above boxplots indicate statistically significant differences among treatments based on one-way ANOVA, followed by Tukey's *post hoc* test ( $p < 0.05$ ). Colors denote sample categories: negative and positive controls (white), soil-derived eluates (brown), ash with vegetation (green), bare weathered ash (grey), and unweathered fly and bottom ash (light grey).

**3.4.2. Genotoxicity of weathered coal ash.** Alongside mitotic inhibition, coal ash exposure induced a variety of chromosomal aberrations in the dividing cells of the root tips. Microscopic observations of chromosomal aberrations revealed that 9 out of 14 samples had significantly higher percentages of cells with chromosomal aberrations, compared to the negative control, with the average chromosomal aberrations (CA) ranging from 0.73% to 26.1%. In comparison, the CA of bulbs treated with the negative and positive controls were 0.72% and 3.34%, respectively (Fig. 6). The highest CA was caused by unweathered fly ash (FA, 26.1%), LP8 (soil, 24.7%), and LŠ7 (soil, 24.2%), while the LŠ1 (soil), LŠ8 (bare), and LP3 (bare) samples did not cause a significant difference in CA.

The spectrum of aberrations included multipolar anaphases, disturbed prophase, lagging and vagrant chromosomes, C-metaphases, anaphase bridges, and chromosomal stickiness (Tables S9, S10 and Fig. 8). This combination of lesion types is consistent with both clastogenic (chromosome-breaking) and

aneugenic (spindle-disrupting) mechanisms.<sup>62</sup> Bridges, fragments and micronuclei are typical of agents that induce DNA strand breaks and misrepair, whereas laggards, C-mitoses and multipolar spindles indicate interference with the mitotic spindle and chromosome segregation.<sup>15,31</sup> Chromosome stickiness, observed in the most affected treatments (especially FA and the most toxic weathered samples), is considered an irreversible alteration of chromatin structure and is frequently associated with cell death.<sup>31</sup> Together, these aberration types indicate that coal ash eluates can both damage the genetic material and disrupt the mitotic apparatus.

After a 24-hour recovery period in clean water, the frequency of chromosomal aberrations decreased in most samples, with values ranging from 2.32% to 18.2% (Fig. 7). Notable reductions were observed in LŠ7 (from 24% to 9%), LP5 (23% to 12%), and LP8 (25% to 13%), indicating partial damage repair and regeneration by healthier dividing cells. However, recovery was incomplete for several treatments. The unweathered fly ash (FA)



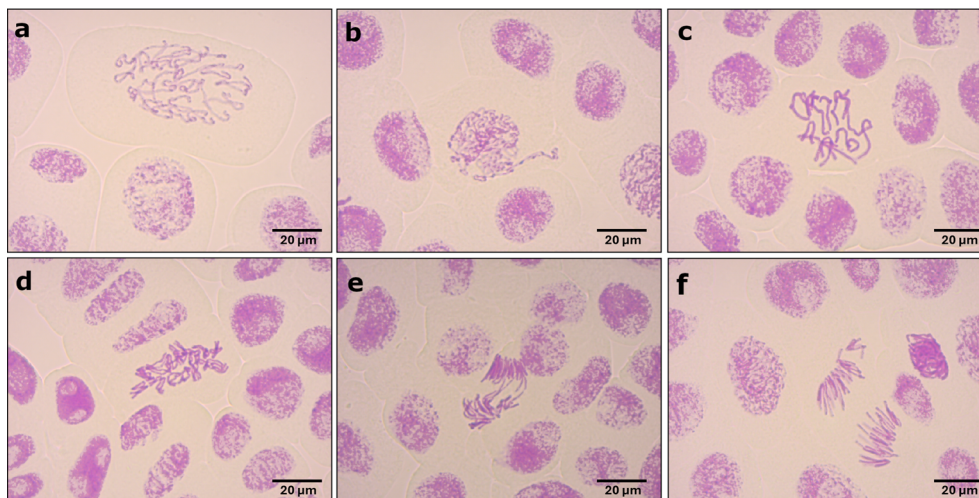


Fig. 8 Some of the observed chromosomal aberrations: (a) disturbed prophase, (b) chromatin erosion, (c) prolonged prophase, (d) spindle disturbance at the metaphase, (e) anaphase bridge and irregular position of the anaphase groups, and (f) chromosomes isolated from the anaphase group.

retained a high aberration rate (~18%), while two bare ash samples (LŠ8 and LP3), as well as the positive control, showed no improvement or even slight increases in CA, suggesting persistent genotoxic effects or delayed manifestation of earlier DNA damage.

Overall, the CA data confirm that both unweathered and weathered coal ash eluates are genotoxic, with the vegetated and soil samples often being more damaging than bare ash at both sites. Because some treatments produced relatively modest MI suppression but strong CA responses (*e.g.*, LP8), while others showed the opposite pattern, chromosomal aberrations should be interpreted jointly with the mitotic index. Taken together, MI and CA reveal that coal ash can induce both acute and residual cytogenetic damage in root meristems, even after a recovery period in clean water.

Data from both mitotic index and percentage of chromosomal aberrations underscore that weathering and revegetation do not universally diminish cytotoxicity and genotoxicity. Even after ~50 years of weathering, many ash samples from both sites retain the capacity to impair cell division and induce genetic damage in plant roots. This finding contrasts with observations by Bandarra *et al.*,<sup>28</sup> who reported relatively low toxicity of decade-old fly ash leachates in several bioassays (with only slight effects on most test organisms). In our case, even ash that had weathered ~50 years, including material from vegetated zones, still contained enough contaminants to significantly impair cell division. This highlights that site-specific factors (such as the original ash composition, coal type, and mode of weathering) can greatly influence the persistence of CCR toxicity.

### 3.5. Linking elemental composition to toxic effects

To identify potential drivers of toxicity in coal ash eluates, correlation analyses were performed separately for Plaški and Štrmac landfills (Fig. 9) to evaluate the potential site-specific

relationship between elemental concentrations (33 detected elements) and biological endpoints: seed germination (SG), relative radicle growth (RRG), mitotic index (MI), and chromosomal aberrations (CA).

In the Plaški eluates, seed germination (SG) decreased with higher levels of Be ( $r = -0.64$ ) and Rb ( $r = -0.42$ ), while Zn ( $r = 0.62$ ) and Ba ( $r = 0.60$ ) showed positive associations. Radicle growth (RG) was negatively associated with Sb ( $-0.68$ ), Li ( $-0.61$ ), and Cs ( $-0.61$ ), but positively linked to Zn (0.72) and Cu (0.48). Mitotic index (MI) was reduced with higher Al ( $-0.67$ ), Cr ( $-0.61$ ), and Ni ( $-0.57$ ), and chromosomal aberrations (CA) increased with V (0.81), As (0.66), and Be (0.60).

Correlation trends in the Štrmac eluates showed both parallels and contrasts. SG correlated positively with Mg (0.81), Co (0.85), and Mn (0.63) but negatively with Cs ( $-0.57$ ) and Cr ( $-0.60$ ). RG had strong positive associations with Be (0.90), Na (0.89), and Mg (0.52) and negative ones with As ( $-0.81$ ) and Fe ( $-0.43$ ). MI decreased with increasing Al ( $-0.60$ ), Ti ( $-0.67$ ), and V ( $-0.63$ ) while showing a slight positive correlation with Cu (0.42). CA was mostly associated with Ti (0.79), V (0.85), and Ca (0.74).

Despite site-specific differences, several elements showed consistent correlations with toxicity endpoints across the Plaški and Štrmac eluates. Al was negatively associated with MI in Plaški ( $r = -0.67$ ) and Štrmac ( $r = -0.60$ ), suggesting mitotic inhibition. As and V showed consistent positive correlations with AI (Plaški: V = 0.81, As = 0.66; Štrmac: V = 0.85, As = 0.43). These recurring patterns point toward a potential role of these elements in driving genotoxic responses.

Correlation alone cannot prove causation; however, the types of chromosomal abnormalities observed in this study (multipolar anaphases, bridges, laggards, stickiness) are consistent with previously described effects of Al, As, and V in root meristems. Al has been shown to interfere with microtubule polymerization and spindle formation, which reduces the mitotic index and produces C-mitosis, sticky chromosomes, and



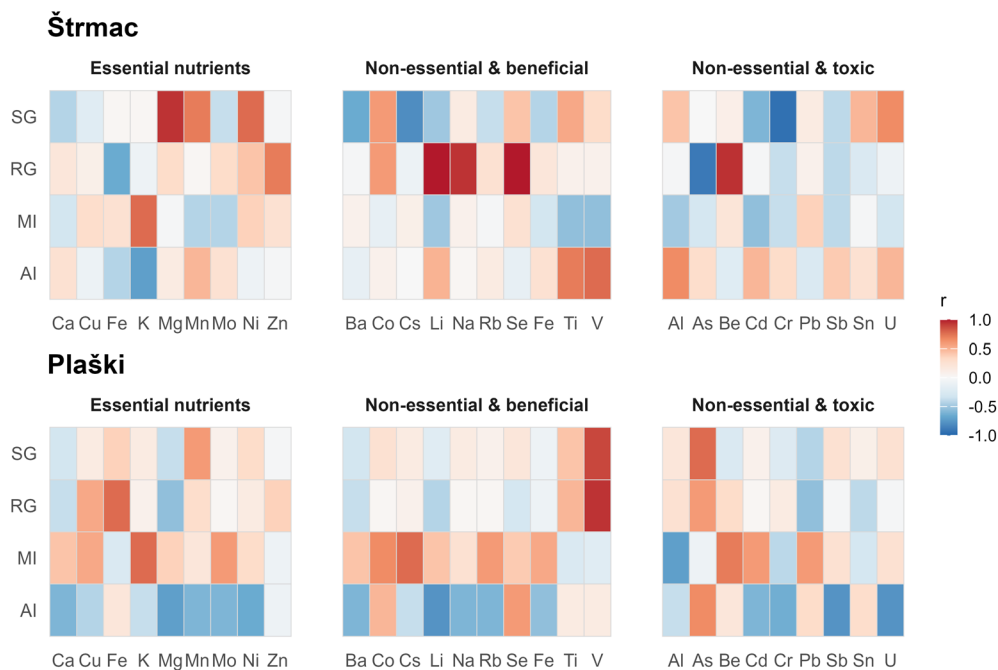


Fig. 9 Correlation heatmap showing relationships between elemental concentrations and bioassay responses—seed germination (SG), radicle growth (RG), mitotic index (MI), and aberration index (AI)—in eluates from weathered coal ash in Štrmac and Plaški. Warm colours (red shade) indicate positive correlations, while cool colours (blue shade) represent negative correlations.

lagging figures.<sup>64</sup> Arsenic primarily exerts genotoxicity through the generation of reactive oxygen species and the disruption of spindle assembly, leading to DNA damage, micronuclei formation, and segregation errors.<sup>65,66</sup> Vanadium, often present as vanadate ( $V^{5+}$ ), can substitute for phosphate in enzymatic processes and disrupt the phosphorylation-dependent steps of mitosis. In addition, it induces oxidative stress, resulting in spindle defects, chromosomal stickiness, and lagging chromosomes.<sup>67,68</sup> Published thresholds for vanadium toxicity in *Allium* roots begin at approximately  $25\text{--}100\ \mu\text{g L}^{-1}$ ,<sup>67,68</sup> which overlaps with the concentrations detected in our eluates.

Importantly, previous leaching experiments conducted on the same CCR materials<sup>27</sup> demonstrated that pedogenetic changes modify the mobility of oxyanion-forming elements, particularly As and V, under the prevailing alkaline to near-neutral pH conditions. These elements exhibit pH-dependent release behaviour, meaning that localized shifts in buffering capacity can enhance their availability in eluates even when total concentrations remain moderate. Thus, the cytogenetic responses observed here are consistent not only with the known cellular mechanisms of Al, As, and V toxicity, but also with their demonstrated mobility in weathered CCR systems. While direct causality cannot be established, the combined geochemical and biological evidence supports their likely contribution to the observed genotoxicity.

Taken together, these mechanisms provide a plausible explanation for the observed cytogenetic effects and support the conclusion that Al, As, and V are among the main contributors to the persistent genotoxicity of weathered CCR eluates.

However, it has to be noted that many elements in coal ash eluates likely act synergistically or antagonistically, which complicates the attribution of specific toxic effects to individual elements.<sup>5</sup>

This is evident in the discrepancy between the elemental concentrations in eluates and the toxic effect of the sample. For example, seven out of twelve eluates significantly inhibited seed germination, including both the soil and bare ash samples from the Plaški (LP3, LP8, LP9, LP10) and Štrmac (LŠ5, LŠ8, LŠ11) landfills. Meanwhile, eluates such as LP3, LP5, LŠ7, LŠ11, and LŠ4 contained trace element concentrations exceeding WHO drinking water thresholds, but not all induced equally strong biological effects. This discrepancy is especially evident in the *Allium* test results: LP1 (vegetated), with moderate elemental content, caused the highest inhibition of cell division ( $MI = 1.94\%$ ), whereas LŠ4 (vegetated) showed no significant impact on mitosis despite exceeding the WHO limit. Similarly, chromosomal aberrations were highest in eluates from fly ash (FA, 26.06%), LP8 (soil, 24.7%), and LŠ7 (soil, 24.2%), while other samples with comparable or higher elemental content, such as LŠ1, LŠ8, and LP3, did not cause significant genotoxicity.

Coal ash is an inherently complex material, often containing various organic and inorganic compounds, as well as dozens of elements across wide concentration ranges and in various chemical forms. The interactions between elements, their competitive uptake by plants, and their speciation in aqueous media can dramatically influence toxicity outcomes. The observed, sometimes contradictory, correlations highlight the need for more detailed chemical characterization in the future, such as speciation modeling or bioavailability assays, to fully



understand the mechanisms of coal ash toxicity. In addition, relying solely on elemental concentrations for coal ash assessment may overlook relevant biological risks, underscoring the value of integrated bioassay approaches. These observations emphasize both the importance and the inherent challenges of assessing CCR toxicity.

### 3.6. Study scope and future perspectives

The present study provides novel insight into the long-term toxicity of approximately 50-year-old weathered CCR under field conditions. However, as with any complex environmental system, certain aspects remain beyond the scope of the current investigation.

The correlation analyses identify statistically robust associations between elemental concentrations and biological endpoints, but they do not allow definitive attribution of toxicity to single elements, as CCR represents a chemically heterogeneous mixture in which multiple components may interact.

In addition, toxicity was evaluated using aqueous eluates and two established plant-based bioassays, which effectively capture early phytotoxic and cytogenetic responses but do not encompass all possible ecological exposure pathways or long-term field effects.

Future research integrating element-specific experimental designs, multi-species testing, and extended field monitoring would further refine our understanding of the mechanisms controlling weathered CCR toxicity. Nevertheless, the combined geochemical and biological approach applied here provides a robust framework for assessing the environmental relevance of legacy coal ash deposits.

## 4. Conclusions

This study demonstrated that weathered coal ash remained phytotoxic even after ~50 years of natural exposure. Both seed germination and *Allium* tests revealed the significant inhibition of growth and cytogenetic damage in eluates from two Croatian landfills, despite evidence of pedogenesis and partial vegetation cover.

Our results show that

(1) Pedogenesis mitigates, but does not eliminate, effects. Vegetated samples generally released fewer trace elements and exhibited weaker toxicity, yet exceptions occurred, particularly for oxyanion-forming elements (As, V, U).

(2) Coal ash continues to impair germination, radicle growth, and cell division, confirming its relevance as a legacy waste.

(3) Correlation analyses identified Al, As, and V as consistent drivers of mitotic inhibition and chromosomal aberrations, supported by known mechanistic pathways. Importantly, the vanadium concentrations in our eluates fall within published toxicological thresholds for *Allium* roots.

(4) Elemental exceedances did not always correspond to the strongest biological responses, reflecting interactions among elements, speciation effects, and bioavailability constraints.

Together, these findings underscore the need to integrate biological endpoints with chemical characterization when assessing the environmental risks of coal ash disposal sites. For effective management and rehabilitation of legacy landfills, monitoring frameworks should move beyond concentration-based thresholds and incorporate bioassays to capture the full spectrum of potential ecological impacts. Such an approach may also be relevant for other waste systems, including mine waste facilities and contaminated soils associated with industrial activities, where complex mixtures can limit the interpretability of chemical data alone, highlighting the value of integrating bioassays in characterisation workflows.

## Conflicts of interest

There are no conflicts to declare.

## Data availability

The data supporting the findings of this study are available in the supplementary information (SI) accompanying this article. Supplementary information: analytical quality-control parameters (limits of detection and control measurements), pH data, total and leachable elemental concentrations, relative mass leached values, seed germination and radicle growth results, *Allium* cytogenetic assay data (mitotic index, chromosomal aberrations, and aberration types), recovery-phase results, and statistical outputs (ANOVA and *post hoc* analyses). See DOI: <https://doi.org/10.1039/d5em01010a>.

## Acknowledgements

This work was supported by the Croatian Science Foundation under the project IP-2019-04-9354 (FORTIS). The authors are grateful to Dr Jasmina Obhodaš for providing the BA and FA samples collected during the 1980s by Dr Vladivoj Valković.

## References

- 1 R. A. Kruger, *Introduction to the Utilization of Coal Combustion Products*, Elsevier Ltd, 2017.
- 2 X. Zhang, Management of coal combustion wastes, [https://usea.org/sites/default/files/012014\\_Managementofcoalcombustionwastes\\_ccc231.pdf](https://usea.org/sites/default/files/012014_Managementofcoalcombustionwastes_ccc231.pdf), accessed 4 March 2026.
- 3 J. Ribeiro, T. F. Silva, J. G. Mendonça Filho and D. Flores, Fly ash from coal combustion - An environmental source of organic compounds, *Appl. Geochem.*, 2014, **44**, 103–110.
- 4 G. Akar, M. Polat, G. Galecki and U. Ipekoglu, Leaching behavior of selected trace elements in coal fly ash samples from Yenikoy coal-fired power plants, *Fuel Process. Technol.*, 2012, **104**, 50–56.
- 5 M. Petrović and Ž. Fiket, Environmental damage caused by coal combustion residue disposal: A critical review of risk assessment methodologies, *Chemosphere*, 2022, **299**, 134410.
- 6 Y. Chen, Y. Fan, Y. Huang, X. Liao, W. Xu, T. Zhang and F. Ash, A comprehensive review of toxicity of coal fly ash



- and its leachate in the ecosystem, *Ecotoxicol. Environ. Saf.*, 2024, **269**, 115905.
- 7 S. M. Raimondo, C. L. Rowe and J. D. Congdon, Exposure to Coal Ash Impacts Swimming Performance and Predator Avoidance in Larval Bullfrogs, *J. Herpetol.*, 1998, **32**, 289–292.
  - 8 C. L. Rowe, O. M. Kinney, A. P. Fiori and J. D. Congdon, Oral deformities in tadpoles (*Rana catesbeiana*) associated with coal ash deposition: Effects on grazing ability and growth, *Freshwater Biol.*, 1996, **36**, 723–730.
  - 9 A. D. Lemly, Selenium poisoning of fish by coal ash wastewater in Herrington Lake, Kentucky, *Ecotoxicol. Environ. Saf.*, 2018, **150**, 49–53.
  - 10 V. E. Mahajan, R. R. Yadav, N. P. Dakshinkar, V. M. Dhoot, G. R. Bhojane, M. K. Naik, P. Shrivastava, P. K. Naoghare and K. Krishnamurthi, Influence of mercury from fly ash on cattle reared nearby thermal power plant, *Environ. Monit. Assess.*, 2012, **184**, 7365–7372.
  - 11 C. H. Zhang, L. Sears, J. V. Myers, G. N. Brock, C. G. Sears and K. M. Zierold, Proximity to coal-fired power plants and neurobehavioral symptoms in children, *J. Exposure Sci. Environ. Epidemiol.*, 2022, **32**, 124–134.
  - 12 R. Kamath, S. E. Udayar, G. Jagadish, P. Prabhakaran, K. K. Madhipatla and Research Team, Assessment of Health Status and Impact of Pollution from Thermal Power Plant on Health of Population and Environment Around the Plant in Udupi District, Karnataka, *Indian J. Public Health.*, 2022, 91–97.
  - 13 M. Karavuş, A. Aker, D. Cebeci, M. Taşdemir, N. Bayram and Ş. Çali, Respiratory Complaints and Spirometric Parameters of the Villagers Living around the Seyitomer Coal-Fired Thermal Power Plant in Kütahya, Turkey, *Ecotoxicol. Environ. Saf.*, 2002, **52**, 214–220.
  - 14 R. Chakraborty, A. K. Mukherjee and A. Mukherjee, Evaluation of genotoxicity of coal fly ash in *Allium cepa* root cells by combining comet assay with the Allium test, *Environ. Monit. Assess.*, 2009, **153**, 351–357.
  - 15 A. Jana, M. Ghosh, S. Sinha, M. Jothiramajayam, A. Nag and A. Mukherjee, Hazard identification of coal fly ash leachate using a battery of cyto-genotoxic and biochemical tests in *Allium cepa*, *Arch. Agron. Soil Sci.*, 2017, **63**, 1443–1453.
  - 16 R. Chakraborty and A. Mukherjee, Mutagenicity and genotoxicity of coal fly ash water leachate, *Ecotoxicol. Environ. Saf.*, 2009, **72**, 838–842.
  - 17 V. L. Markad, K. M. Kodam and V. S. Ghole, Effect of fly ash on biochemical responses and DNA damage in earthworm, *Dichogaster curgensis*, *J. Hazard. Mater.*, 2012, **215–216**, 191–198.
  - 18 B. Sambandam, T. Devasena, V. I. Hairul Islam and B. M. Prakhya, Characterization of coal fly ash nanoparticles and their induced in vitro cellular toxicity and oxidative DNA damage in different cell lines, *Indian J. Exp. Biol.*, 2015, **53**, 585–593.
  - 19 P. K. Singh, P. Tripathi, S. Dwivedi, S. Awasthi, M. Shri, D. Chakraborty and R. D. Tripathi, Fly-ash augmented soil enhances heavy metal accumulation and phytotoxicity in rice (*Oryza sativa* L.); A concern for fly-ash amendments in agriculture sector, *Plant Growth Regul.*, 2016, **78**, 21–30.
  - 20 V. L. Markad, S. S. Adav, V. S. Ghole, S. K. Sze and K. M. Kodam, Proteomics study revealed altered proteome of *Dichogaster curgensis* upon exposure to fly ash, *Chemosphere*, 2016, **160**, 104–113.
  - 21 A. P. Crnić, D. Damijanić, N. Bilandžić, M. Sedak and G. Medunić, Enhanced levels of hazardous trace elements (Cd, Cu, Pb, Se, Zn) in bird tissues in the context of environmental pollution by Raša coal, *Rud.-Geol.-Naftni Zb.*, 2022, **37**, 19–30.
  - 22 S. Radić, G. Medunić, Ž. Kuharić, V. Roje, K. Maldini, V. Vujčić and A. Krivohlavek, The effect of hazardous pollutants from coal combustion activity: Phytotoxicity assessment of aqueous soil extracts, *Chemosphere*, 2018, **199**, 191–200.
  - 23 Y. Cui, Y. G. Zhu, R. Zhai, Y. Huang, Y. Qiu and J. Liang, Exposure to metal mixtures and human health impacts in a contaminated area in Nanning, China, *Environ. Int.*, 2005, **31**, 784–790.
  - 24 S. Mortazavi, G. Mortazavi and M. Paknahad, Levels of arsenic, mercury, cadmium, copper, lead, zinc, and manganese in serum and whole blood of resident adults from mining and non-mining communities in Ghana, *Environ. Sci. Pollut. Res.*, 2016, **23**, 22220–22221.
  - 25 Ł. Uzarowicz, Z. Zagórski, E. Mendak, P. Bartmiński, E. Szara, M. Kondras, L. Oktaba, A. Turek and R. Rogoziński, Technogenic soils (Technosols) developed from fly ash and bottom ash from thermal power stations combusting bituminous coal and lignite. Part I. Properties, classification, and indicators of early pedogenesis, *Catena*, 2017, **157**, 75–89.
  - 26 M. Petrović, M. Ivanić, N. Vdović, M. Dolenc, B. Čermelj, P. Šket, G. Medunić and Ž. Fiket, Physicochemical and mineral characteristics of soil materials developed naturally on two ~ 50 years old coal combustion residue disposal sites in Croatia, *Catena*, 2023, **231**, 107338.
  - 27 M. Petrović, A. Ninčević Grassino, J. Lapić, S. Djaković, M. Furdek Turk, G. Medunić and Ž. Fiket, Changes in the mobility of oxyanions from coal combustion residues after 50 years of natural weathering, *Waste Manage.*, 2026, **216**, 115450.
  - 28 B. S. Bandarra, L. A. Gomes, J. L. Pereira, F. J. M. Gonçalves, R. C. Martins and M. J. Quina, Assessment of hazardous property HP 14 using ecotoxicological tests: a case study of weathered coal fly ash, *Environ. Sci. Pollut. Res.*, 2020, **27**, 20972–20983.
  - 29 R. J. Haynes, Reclamation and revegetation of fly ash disposal sites - Challenges and research needs, *J. Environ. Manage.*, 2009, **90**, 43–53.
  - 30 G. Fiskesjö, in *Environmental Toxicology and Risk Assessment: 2nd Volume, American Society for Testing and Materials*, ed. J. W. Gorsuch, F. J. Dwyer, C. G. Ingersoll and T. W. La Point, STP 1216, Philadelphia, 1993, pp. 331–345.
  - 31 G. Fiskesjö, The Allium test as a standard in environmental monitoring, *Hereditas*, 1985, **102**, 99–112.
  - 32 Y. Luo, J. Liang, G. Zeng, M. Chen, D. Mo, G. Li and D. Zhang, Seed germination test for toxicity evaluation of



- compost: Its roles, problems and prospects, *Waste Manage.*, 2018, **71**, 109–114.
- 33 G. Medunić, A. Radenović, M. Bajramović, M. Švec and M. Tomac, Once grand, now forgotten: What do we know about the superhigh-organic-sulphur Raša coal?, *Rud.-Geol.-Naftni Zb.*, 2016, **31**, 27–45.
- 34 G. Medunic, Ž. Kuharic, A. Krivohlavek, Ž. Fiket, A. Radenovic, K. Gödel, Š. Kampic and G. Kniewald, Geochemistry of Croatian superhigh-organic-sulphur Raša coal, imported low-S coal and bottom ash: Their se and trace metal fingerprints in seawater, clover, foliage and mushroom specimens copyright, *Int. J. Oil, Gas Coal Technol.*, 2018, **18**, 3–24.
- 35 Ž. Fiket, G. Medunić, Ž. Vidaković-Cifrek, P. Jezidžić and P. Cvjetko, Effect of coal mining activities and related industry on composition, cytotoxicity and genotoxicity of surrounding soils, *Environ. Sci. Pollut. Res.*, 2020, **27**, 6613–6627.
- 36 G. Medunić, M. Ahel, I. B. Mihalić, V. G. Srček, N. Kopjar, Ž. Fiket, T. Bituh and I. Mikac, Toxic airborne S, PAH, and trace element legacy of the superhigh-organic-sulphur Raša coal combustion: Cytotoxicity and genotoxicity assessment of soil and ash, *Sci. Total Environ.*, 2016, **566–567**, 306–319.
- 37 V. Oreščanin, R. Kollar, K. Buben, I. L. Mikelic, K. Kollar, M. Kollar and G. Medunic, Chemical and radiological characterization of fly and bottom ash landfill of the former sulfate pulp factory Plaški and its surroundings, *J. Environ. Sci. Health, Part A: Toxic/Hazard. Subst. Environ. Eng.*, 2012, **47**, 1592–1606.
- 38 J. Weber, S. Straczyńska, A. Kocowicz, M. Gilewska, A. Bogacz, M. Gwizdz and M. Debicka, Properties of soil materials derived from fly ash 11 years after revegetation of post-mining excavation, *Catena*, 2015, **133**, 250–254.
- 39 CEN, Characterization of waste–Leaching–Compliance test for leaching of granular waste material and sludge. Part 2: One stage batch test at a liquid to solid ratio of 10 L/kg with article size below 4 mm (without or with size reduction). EN 12457–2, Brussels, 2002.
- 40 European Commission, Council Decision 2003/33/EC of 19 December 2002 establishing criteria and procedures for the acceptance of waste at landfills pursuant to Article 16 and Annex II of Directive 1999/31/EC, <https://eur-lex.europa.eu/legal-content/EN/TXT/?uri=CELEX:32003D0033%0A%0A>.
- 41 World Health Organization, *Guidelines for Drinking-Water Quality*, World Health Organization, Geneva, 4th edn, 2022.
- 42 D. Fritz, A. P. Bernardi, J. S. Haas, B. M. Ascoli, S. A. L. De Bordignon and G. Von Poser, Germination and growth inhibitory effects of *Hypericum myrianthum* and *H. polyanthum* extracts on *Lactuca sativa* L., *Rev. Bras. Farmacogn.*, 2007, **17**, 44–48.
- 43 A. K. Sharma and A. Sharma, *Chromosome Techniques: Theory and Practice*, Butterworths & Co Ltd, London, 2nd edn, 1972.
- 44 N. Moreno, X. Querol, J. M. Andrés, K. Stanton, M. Towler, H. Nugteren, M. Janssen-Jurkovicová and R. Jones, Physico-chemical characteristics of European pulverized coal combustion fly ashes, *Fuel*, 2005, **84**, 1351–1363.
- 45 N. R. Lieberman, M. Izquierdo, C. Muñoz-Quirós, H. Cohen and S. R. Chenery, Geochemical signature of superhigh organic sulphur Raša coals and the mobility of toxic trace elements from combustion products and polluted soils near the Plomin coal-fired power station in Croatia, *Appl. Geochem.*, 2020, **114**, 104472.
- 46 M. Petrović, Ž. Fiket, G. Medunić and S. Chakravarty, Mobility of metals and metalloids from SHOS coal ash and slag deposit: mineralogical and geochemical constraints, *Environ. Sci. Pollut. Res.*, 2022, **29**, 46916–46928.
- 47 P. Suraneni, L. Burris, C. R. Shearer and R. D. Hooton, ASTM C618 fly ash specification: Comparison with other specifications, shortcomings, and solutions, *ACI Mater. J.*, 2021, **118**, 157–167.
- 48 M. P. Ketris and Y. E. Yudovich, Estimations of Clarkes for Carbonaceous biolithes: World averages for trace element contents in black shales and coals, *Int. J. Coal Geol.*, 2009, **78**, 135–148.
- 49 G. Faure, *Principles and Applications of Geochemistry: a Comprehensive Textbook for Geology Students*, Prentice-Hall, Inc., 2nd edn, 1998.
- 50 P. Marschner, *Marschner's Mineral Nutrition of Higher Plants*, 2012.
- 51 M. Izquierdo and X. Querol, Leaching behaviour of elements from coal combustion fly ash: An overview, *Int. J. Coal Geol.*, 2012, **94**, 54–66.
- 52 S. Zhao, Z. Chen, J. Shen, J. Kang, J. Zhang and Y. Shen, Leaching mechanisms of constituents from fly ash under the influence of humic acid, *J. Hazard. Mater.*, 2017, **321**, 647–660.
- 53 B. Dold and L. Fontboté, A mineralogical and geochemical study of element mobility in sulfide mine tailings of Fe oxide Cu-Au deposits from the Punta del Cobre belt, northern Chile, *Chem. Geol.*, 2002, **189**, 135–163.
- 54 O. Kostić, S. Jarić, G. Gajić, D. Pavlović, M. Pavlović, M. Mitrović and P. Pavlović, Pedological properties and ecological implications of substrates derived 3 and 11 years after the revegetation of lignite fly ash disposal sites in Serbia, *Catena*, 2018, **163**, 78–88.
- 55 X. Wang, H. A. van der Sloot, K. G. Brown, A. C. Garrabrants, Z. Chen, B. Hensel and D. S. Kosson, Application and uncertainty of a geochemical speciation model for predicting oxyanion leaching from coal fly ash under different controlling mechanisms, *J. Hazard. Mater.*, 2022, **438**, 129518.
- 56 S. M. Tiquia, N. F. Y. Tam and I. J. Hodgkiss, Effects of composting on phytotoxicity of spent pig-manure sawdust litter, *Environ. Pollut.*, 1996, **93**, 249–256.
- 57 A. Fuentes, M. Lloréns, J. Sáez, M. I. Aguilar, J. F. Ortuño and V. F. Meseguer, Phytotoxicity and heavy metals speciation of stabilised sewage sludges, *J. Hazard. Mater.*, 2004, **108**, 161–169.
- 58 R. Karlova, D. Boer, S. Hayes and C. Testerink, Root plasticity under abiotic stress, *Plant Physiol.*, 2021, **187**, 1057–1070.
- 59 H. Q. Wang, X. Y. Zhao, W. Xuan, P. Wang and F. J. Zhao, Rice roots avoid asymmetric heavy metal and salinity



- stress via an RBOH-ROS-auxin signaling cascade, *Mol. Plant*, 2023, **16**, 1678–1694.
- 60 E. R. Emينو and P. R. Warman, Biological Assay for Compost Quality, *Compost Sci. Util.*, 2004, **12**, 342–348.
- 61 D. M. Leme and M. A. Marin-Morales, *Allium cepa* test in environmental monitoring : A review on its application, *Mutat. Res., Rev. Mutat. Res.*, 2009, **682**, 71–81.
- 62 D. M. Leme and M. A. Marin-Morales, *Allium cepa* test in environmental monitoring : A review on its application, *Mutat. Res., Rev. Mutat. Res.*, 2009, **682**, 71–81.
- 63 S. Gantayat, S. Mania, C. Pradhan and A. B. Das, Ionic Stress Induced Cytotoxic Effect of Cadmium and Nickel Ions on Roots of *Allium cepa* L, *Cytologia*, 2018, **83**, 143–148.
- 64 D. Liu, W. Jiang and D. Li, Effects of aluminium ion on root growth, cell division, and nucleoli of garlic (*Allium sativum* L.), *Environ. Pollut.*, 1993, **82**, 295–299.
- 65 L. Wu, H. Yi and M. Yi, Assessment of arsenic toxicity using *Allium/Vicia* root tip micronucleus assays, *J. Hazard. Mater.*, 2010, **176**, 952–956.
- 66 H. Yi, L. Wu and L. Jiang, Genotoxicity of arsenic evaluated by *Allium-root* micronucleus assay, *Sci. Total Environ.*, 2007, **383**, 232–236.
- 67 L. Marcano, I. Carruyo, Y. Fernández, X. Montiel and Z. Torrealba, Determination of vanadium accumulation in onion root cells (*Allium cepa* L.) and its correlation with toxicity, *Biocell*, 2006, **30**, 259–267.
- 68 M. Kaya, K. Çavuşoğlu, E. Yalçın and A. Acar, DNA fragmentation and multifaceted toxicity induced by high-dose vanadium exposure determined by the bioindicator *Allium* test, *Sci. Rep.*, 2023, **13**, 1–11.

